Adsorption of polyvinyl alcohol from wastewater by sintered porous red mud

Yihe Zhang, Wei Chen, Guocheng Lv, Fengzhu Lv, Paul K. Chu, Wenmin Guo, Baolin Cui, Rui Zhang and Hell Wang

ABSTRACT

Several types of red mud-based porous materials (RMPM) and other raw minerals via different processes were prepared and characterized using X-ray diffraction (XRD) analyses and scanning electron microscope (SEM) observations. Using the polymer sponge method, a 72% apparent porosity could be reached compared with 64% by adding a pore-forming agent. These materials were tested for their adsorption of polyvinyl alcohol (PVA) from simulated textile wastewater. The best mass ratio of RMPM to PVA solution was 50:100 with a removal maximum of 25.8% after they were in contact for 50 min. The adsorption rate and kinetics could be better described by Lagergren's pseudo-second-order model in comparison with the pseudo-first-order model.

Key words | adsorption, porous materials, PVA, red mud

Yihe Zhang (corresponding author)
Wei Chen
Guocheng Lv
Fengzhu Lv
Wenmin Guo
Baolin Cui
Rui Zhang
State Key Laboratory of Geological Processes & Mineral Resources,
National Laboratory of Mineral Materials,
School of Materials Science and Technology,
China University of Geosciences (Beijing),
Beijing, 100083,
China
E-mail: *zyh@cugb.edu.cn*

Yihe Zhang
Paul K. Chu
Department of Physics & Materials Science,
City University of Hong Kong,
Tat Chee Avenue, Kowloon, Hong Kong,
China

Heli Wang
School of Water Resources and Environment,
China University of Geosciences (Beijing),
Beijing, 100083,
China

INTRODUCTION

Red mud, called bauxite residue, is a solid state industrial byproduct produced during alumina extraction from bauxite. About 70 Mt of dry red mud are produced by the alumina industry annually. The waste which typically ends up in red mud landfill leads to deleterious effects such as devastated cropland, polluted surface water and local environment, as well as expensive maintenance. Therefore, much effort is being made to effectively recycle the red mud waste. One of these applications is to remove microorganisms, inorganic and organic contaminants from wastewater (Weaver & Ritchie 1987; Ho *et al.* 1991; Ho *et al.* 1992; Lopez *et al.* 1998). However, efforts so far have concentrated on raw red mud and organic contaminants such as viruses and small molecules. Red mud is potentially useful to ceramic filter media and the cement and building industry (Brown & Beretka 1984; Tsakiridis *et al.* 2004) and plastic fillers, as well as in other applications (Boufounos 2005; Liu *et al.* 2009). Moreover, the red mud-based porous materials (RMPM) can be utilized in wastewater treatment in two aspects, as a substitute for filtration materials in advanced water treatment and as carriers of microbes (Xiao *et al.* 2007).

Utilization of red mud in ceramic production has attracted much interest, especially production of red mud ceramic by RMPM sintering. The required strength could be achieved by sintering it at 950 °C for over 48 h at a pressure of 5,000 kg m^{-2} (Prasad & Sharma 1986). A higher sintering temperature of 1,100–1,200 °C was also suggested (Moya *et al.* 1987; Perez *et al.* 1999). The disadvantages of these materials are the large shrinkage and minimum water adsorption.

Polyvinyl alcohol (PVA), a sizing agent used in the textile and printing industry, was the main pollutant in industrial wastewater. Three main processes, Fenton oxidation process (Lin & Lo 1997; Hachem *et al.* 2001; Georgiou *et al.* 2002; Baban *et al.* 2003; Selcuk *et al.* 2003), ultra filtration membrane technology (Lin & Lan 1995; Porter 1998; Ji *et al.* 2006), and biochemical method (Ugoji

doi: 10.2166/wst.2012.114

& Aboaba 2004; Ranganathan *et al*. 2007), were proposed to treat the PVA containing wastewater. To the best of our knowledge, the use of RMPM in treating PVA containing wastewater has not been reported. In this study, the RMPM with a porous structure and high specific area was prepared by incorporating fly ash and bentonite powders to enhance the strength and porosity and the feasibility of using the RMPM for wastewater treatment was assessed.

MATERIALS AND METHODS

Materials

The red mud was an industrial by-product provided by Shandong Weiqiao Pioneering Group Co. Ltd. The fly ash was supplied by the Beijing Gaojing power plant and the bentonite and coal were purchased from Chifeng Fulong Mineral Resource Development Co. Ltd. in Inner Mongolia. All raw materials were ground to 200 meshes and dried at 100 °C for 12 h prior to use. The PVA (CP) was purchased from Beijing Chemical Plant and dried at 100 °C for 24 h before use.

Preparation of RMPM

The pore-forming agent method and polymer sponge technique were adopted. The materials were prepared with red mud, fly ash, bentonite, and foaming additive at the weight rate of 10:5:4:n (n being an integer between 1 and 10). Calcium carbonate ($CaCO_3$) and coal powders were used individually and together with the pore-forming agent. After powders being mixed uniformly, molding, drying, and sintering were conducted sequentially. Sintering was the most important step in these processes and the typical sintering process curve of the porous materials is shown in Figure 1. The sintering technology included three steps: heat treatment, dehydration, and sintering at a higher temperature. After cooling in a furnace, the RMPM balls were produced.

Characterization of RMPM

The apparent porosity was measured by the boiling method according to the Chinese National Standard GB/T 1966–1996. The measurements were carried out after keeping the samples in an oven at 100 °C for 24 h. X-ray powder diffraction (XRD) patterns were acquired for the red mud and RMPM on a Rigaku X-ray diffractometer with Cu K_α radiation (2 kV rotating anode, $\lambda = 1.54056$Å) at 40 kV, 100 mA, and a scanning rate of 2 degrees per min. The surface morphology was examined by scanning electron microscopy (SEM, JEOL JSM-6300) on the gold coated samples.

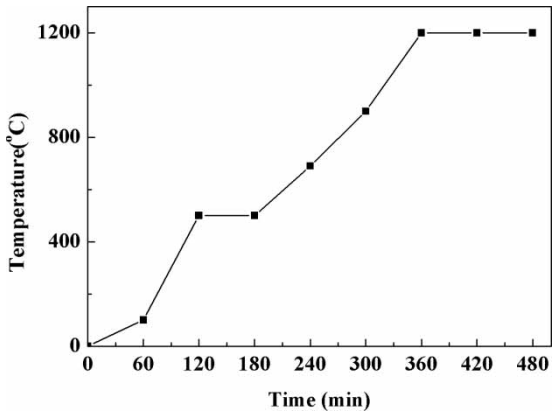

Figure 1 | Sintering processing curve for the RMPM.

The measurement of concentration of PVA solution

The concentration of PVA was determined using a 722 sp-type VIS-Spectrophotometer. PVA reacted with an I_2-KI solution in boric acid to form a complex which exhibited selective absorption at 640 nm. A series of solutions with known PVA concentrations were first reacted and appropriate amounts of the I_2-KI and boric acid solutions were added to blue-green solution. The absorbance values at 640 nm were recorded and the relationship between absorbance and PVA concentrations was fitted.

RESULTS AND DISCUSSION

Effect of foaming agent and process on the porosity of RMPM

Based on the results acquired from a series of RMPM prepared by different processes, the apparent porosity can reach 64% by adding 40 wt% coal powders as the pore-forming agent (marked as A-RMPM), whereas it is 72% by adopting the polymer sponge method (marked as B-RMPM) (Figure 2).

The foaming capability of coal powders is much higher than that of $CaCO_3$ for the same filling content (Figure 2). It could be attributed to the amount of gas produced from the coal powders, which was higher than that from $CaCO_3$

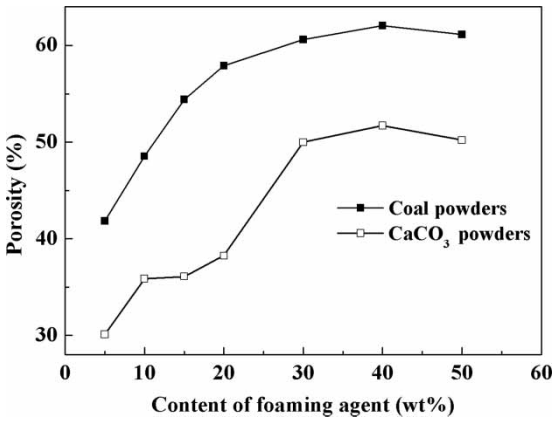

Figure 2 | Effects of foaming agent on the porosity of RMPM.

during sintering when the mass was equal. In addition, the RMPM made with $CaCO_3$ had more closed gas pores which could not be detected by the apparent porous measurement.

SEM morphology of RMPM

The morphology of the RMPM produced by the polymer sponge method revealed an apparent duct structure (Figure 3 (a)). The gas pores on the fractured surface of the RMPM containing 40 wt% $CaCO_3$ were closed (Figure 3(b)), while the gas pores in the RMPM containing 40 wt% coal were interconnected with each other (Figure 3(c)).

X-ray diffraction analysis of RMPM

Crystallization that occurs during sintering is one of the main factors affecting the strength of the RMPM. By adding 40 wt% of coal powders to the raw materials, a new phase of anorthite, $(Ca,Na)(Si,Al)_4O_8$, was formed (Figure 4(b)). On the other hand, additional new phases of calcium silicate Ca_2SiO_4 and calcium aluminium oxide $Ca_3Al_2O_6$ were formed when $CaCO_3$ was introduced (Figure 4(c)). These two minerals usually exist in concrete and contribute to the hardness and toughness of the materials. The two new phases anorthite ($CaAl_2Si_2O_8$) and calcium aluminium oxide $Ca_3Al_2O_6$ were formed for the RMPM containing 15% coal powders and 5% $CaCO_3$ (Figure 4(d)), implying that the RMPM samples containing $CaCO_3$ and coal powders possess good hardness and strength. In addition, proper addition of $CaCO_3$ can deplete Fe_2O_3, which matches the colour changes observed from the RMPM (Figures 4(a), (c), and (d)). The RMPM sample containing 40 wt% $CaCO_3$ is whiter than the other ones due to the disappearance of red Fe_2O_3.

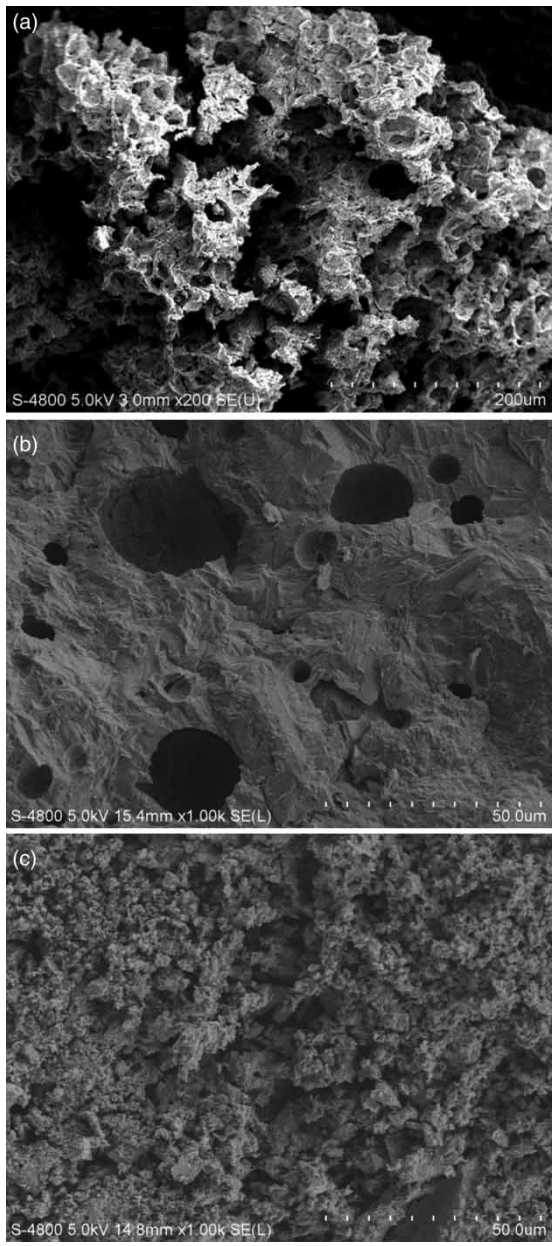

Figure 3 | (a) SEM picture of the RMPM produced by the polymer sponge method; (b) SEM picture of the RMPM containing 40 wt% $CaCO_3$; (c) SEM picture of the RMPM containing 40 wt% coal powders.

Effect of RMPM content on the removal of PVA

Two types of RMPM were applied to the treatment of PVA-containing wastewater. The simulated wastewater was produced by dissolving pure PVA at a concentration of 3.109 mg L^{-1}. Different amounts of RMPM (5–35 mg) were added to 40 mL of the simulated wastewater. A better removal could be achieved by B-RMPM in comparison with A-RMPM (Figure 5).

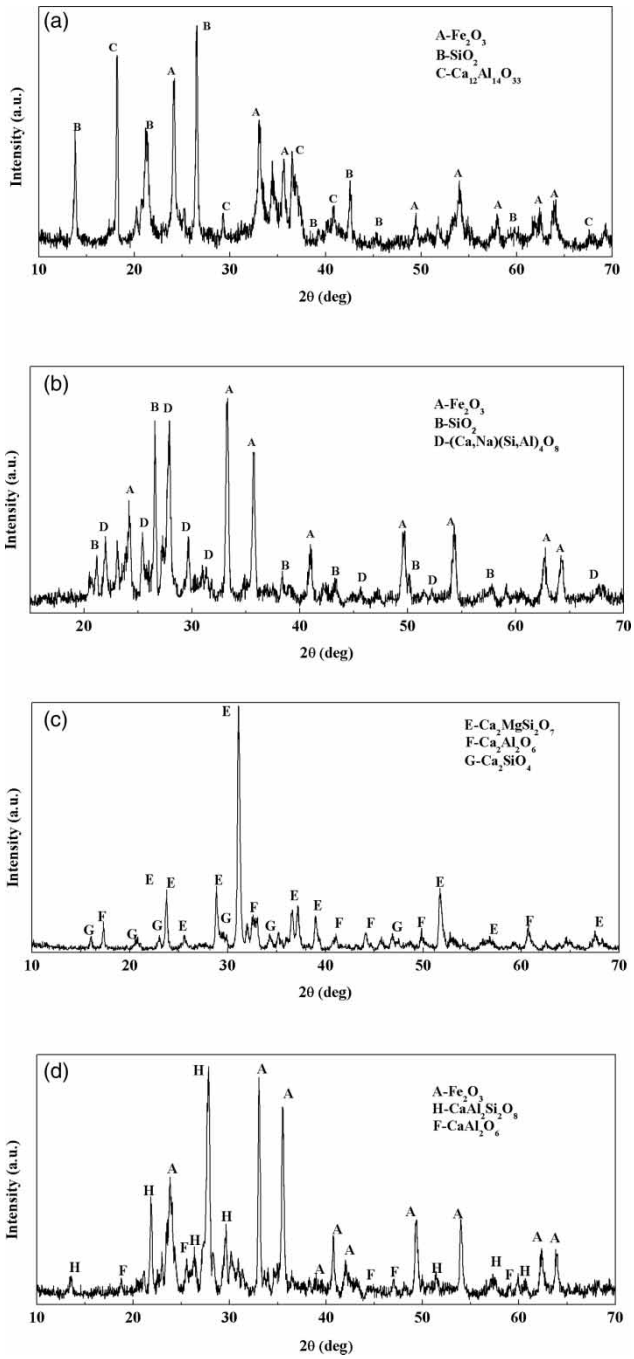

Figure 4 | (a) X-ray powder diffraction pattern obtained from the red mud; (b) X-ray powder diffraction pattern of the RMPM containing 40 wt% coal powders; (c) X-ray powder diffraction pattern acquired from the RMPM containing 40 wt % $CaCO_3$; (d) X-ray powder diffraction pattern of the RMPM containing 15 wt% coal powders and 5 wt% $CaCO_3$.

The PVA concentration decreases as the RMPM mass increases. Adsorption began to saturate at 20 mg for B-RMPM and 25 mg for A-RMPM. Furthermore, B-RMPM could absorb more PVA and reach saturation faster than A-RMPM, due to its larger porosity and interconnected porous structure of B-RMPM as demonstrated by the SEM picture.

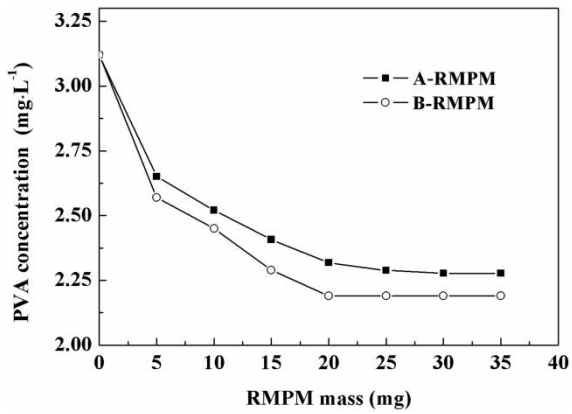

Figure 5 | Effect of RMPM mass on PVA removal.

Effect of adsorption time on the removal of PVA

The concentration of PVA decreases with time (Figure 6). Adsorption saturation occurred at about 60 and 50 min of exposure to simulated wastewater for A-RMPM and B-RMPM, respectively. The higher porosity of B-RMPM resulted in a faster adsorption in the initial 10 min and PVA removal of PVA reached the maximum of 25.8% after 50 min. The low efficiency may be attributed to the larger molecule size and higher viscosity of PVA that prevented more PVA molecules from adsorbing onto the fine pore space of the RMPM.

Kinetic modelling

Two simplified kinetic models, namely the pseudo-first-order model and pseudo-second-order model (Zheng

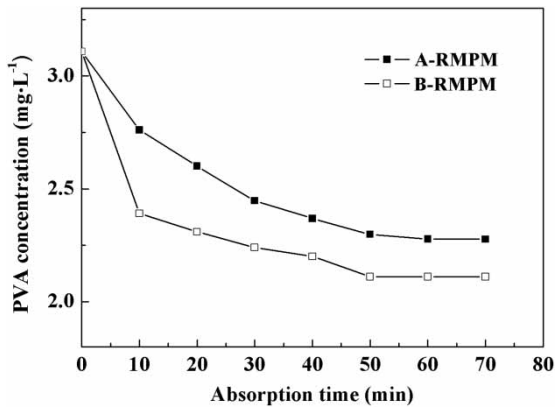

Figure 6 | Effect of adsorption time on PVA removal.

et al. 2008, 2009; Guo *et al.* 2010), were employed to study the rate and kinetics of adsorption of PVA onto RMPM. The Lagergren's rate equation was used to describe the adsorption of an adsorbate from the liquid phase. The linear form of the pseudo-first-order rate expression is given as:

$$\log(q_e - q_t) = \log q_e - \frac{K_f}{2.303}t$$

where q_e and q_t represent the amounts of absorbed PVA (mg g^{-1}) at equilibrium and at time t (min), respectively, and k_f is the rate constant of the pseudo-first-order process. The linear form of the pseudo-second-order rate expression of Lagergren is given as:

$$\frac{t}{q_t} = \frac{1}{k_s q_e^2} + \frac{1}{q_e}t$$

where k_s is the rate constant in the pseudo-second-order process. The linearized plots of the pseudo-first-order and pseudo-second-order kinetic models for A-RMPM and B-RMPM are illustrated in Figures 7 and 8, respectively.

The pseudo-first-order model was not suitable due to a lower correlation coefficient (<0.93) (Figure 7). In contrast, good linearity with a good correlation coefficient of >0.99 for B-RMPM was achieved (Figure 8), indicating the applicability of the pseudo-second-order model to this study. The pseudo-second-order rate constants determined from the slope and intercept in Figure 8 are shown in Table 1.

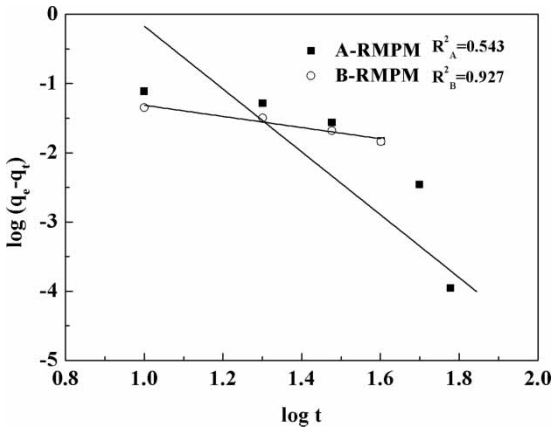

Figure 7 | Adsorption of PVA on A-RMBM and B-RMBM based on pseudo-first-order kinetics.

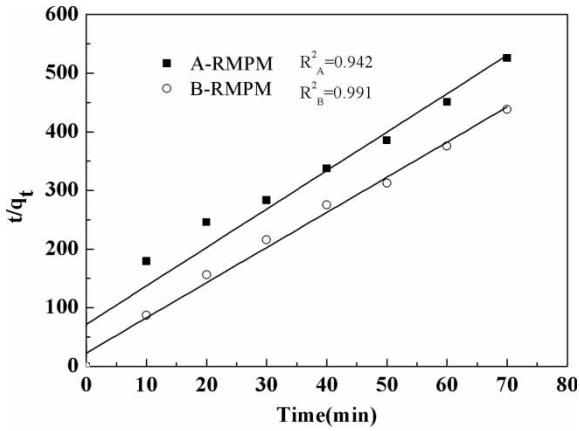

Figure 8 | Absorption of PVA on A-RMBM and B-RMBM based on pseudo-second-order kinetics.

Table 1 | Parameters in the pseudo-second-order model

	C_0 (mg L^{-1})	q_e (mg g^{-1})	k_s (g mg min^{-1})	R^2
A-RMPM	3.11	0.15	1.58	0.94
B-RMPM	3.11	0.17	0.60	0.99

CONCLUSIONS

RMPM with a mass ratio of red mud, fly ash, bentonite to foaming additive of 10:5:4:n (n being an integer between 1 and 10) are produced. Two methods are adopted in the production of RMPM. The B-RMPM samples fabricated by the polymer sponge method have larger porosity than A-RMPM samples made by the pore-forming agent method. When the two RMPM samples are exposed to simulated PVA-containing wastewater, B-RMPM exhibits a higher efficiency than A-RMPM. Adsorption of PVA by B-RMPM not only is quicker but also shows a larger capacity. The concentration of the simulated PVA wastewater decreases with increasing weights of B-RMPM or A-RMPM. The adsorption rate and kinetics fit the Lagergren's pseudo-second-order model better than the pseudo-first-order model.

ACKNOWLEDGEMENTS

The work was jointly supported by the Fundamental Research Funds for the Central Universities (2010ZD08) the open foundation of National Laboratory of Mineral Materials of China University of Geosciences (Grant No. 519002310062 08A003 and 08A004), the Key Project of

Chinese Ministry of Education (No:107023), Special fund of Co-construction of Beijing Education Committee, and City University of Hong Kong Strategic Research Grant (SRG) No. 7008009.

REFERENCES

Baban, A., Yediler, A., Lienert, D., Kemerder, N. & Kettrup, A. 2003 Ozonation of high strength segregated effluents from a woolen textile dyeing and finishing plant. *Dyes and Pigments* **58** (2), 93–98.

Boufounos, D. 2005 Alternative applications for bauxite residue. In: *Proc. 1st Hellenic Conf. for the Utilization of By-Products in Construction*. Thessaloniki, 153, pp. 183–190.

Brown, T. & Beretka, J. 1984 Red mud as a raw material for the heavy clay industry. *Ceramurgia* **14** (4), 155–160.

Georgiou, D., Melidis, P., Aivasidis, A. & Gimouhopoulos, K. 2002 Degradation of azo-reactive dyes by ultraviolet radiation in the presence of hydrogen peroxide. *Dyes and Pigments* **52** (2), 69–78.

Guo, H., Li, Y. & Zhao, K. 2010 Arsenate removal from aqueous solution using synthetic siderite. *Journal of Hazardous Materials* **176** (1–3), 174–180.

Hachem, C., Bocquillon, F., Zahraa, O. & Bouchy, M. 2001 Decolourization of textile industry wastewater by the photocatalytic degradation process. *Dyes and Pigments* **49** (2), 117–125.

Ho, G. E., Gibbs, R. A. & Mathew, K. 1991 Bacteria and virus removal from secondary effluent in sand and red mud columns. *Water Science and Technology* **23** (1–3), 261–270.

Ho, G. E., Mathew, K. & Gibbs, R. A. 1992 Nitrogen and phosphorus removal from sewage effluent in amended sand columns. *Water Research* **26** (3), 295–300.

Ji, Z. J., He, Y. S. & Zhang, G. J. 2006 Treatment of wastewater during the production of reactive dyestuff using a spiral nanofiltration membrane system. *Desalination* **201** (1–3), 255–266.

Lin, S. H. & Lan, W. J. 1995 Polyvinyl alcohol recovery by ultrafiltration: effects of membrane type and operating conditions. *Separations Technology* **5** (2), 97–103.

Lin, S. H. & Lo, C. C. 1997 Fenton process for treatment of desizing wastewater. *Water Research* **31** (8), 2050–2056.

Liu, W. C., Yang, J. K. & Xiao, B. 2009 Application of Bayer red mud for iron recovery and building material production from alumosilicate residues. *Journal of Hazardous Materials* **161** (1), 474–478.

Lopez, E., Soto, B. & Arias, M. 1998 Adsorbent properties of red mud and its use for wastewater treatment. *Water Research* **32** (4), 1314–1322.

Moya, J. S., Morales, F. & Garcia, V. A. 1987 Ceramic use of red mud from alumina plants. *Bol. Soc. Esp. Ceram. V.* **26**, 21–29.

Perez, R. G. A., Guitian, R. F. & Aza Pendas, S. De 1999 Industrial obtaining of ceramic materials from the Bayer process red mud's. *Bol. Soc. Esp. Ceram* **38**, 220–226.

Porter, J. J. 1998 Recovery of polyvinyl alcohol and hot water from the textile wastewater using thermally stable membranes. *Journal of Membrane Science* **151** (1), 45–53.

Prasad, P. M. & Sharma, J. M. 1986 Characterization of and applications for an Indian red mud. *Proceedings of Electrometallurgy* **24**, 12–23.

Ranganathan, K., Jeyapaul, S. & Sharma, D. C. 2007 Assessment of water pollution in different bleaching based paper manufacturing and textile dyeing industries in India. *Environmental Monitoring and Assessment* **134** (1–3), 363–372.

Selcuk, H., Sene, J. J. & Anderson, M. A. 2003 Photoelectrocatalytic humic acid degradation kinetics and effect of pH, applied potential and inorganic ions. *Journal of Chemical Technology and Biotechnology* **78** (9), 979–984.

Tsakiridis, P. E., Agatzini-Leonardou, S. & Oustadakis, P. 2004 Red mud addition in the raw meal for the production of Portland cement clinker. *Journal of Hazardous Materials* **116** (1–2), 103–110.

Ugoji, E. O. & Aboaba, O. O. 2004 Biological treatments of textile industrial effluents in Lagos metropolis, Nigeria. *Journal of Environmental Biology* **25** (4), 497–502.

Weaver, D. M. & Ritchie, G. S. P. 1987 The effectiveness of lime-based amendments and bauxite residues at removing phosphorus from piggery effluent. *Environmental Pollution* **46** (3), 163–175.

Xiao, B., Wu, Sh. B., Shi, X. Y. & Yang, J. K. 2007 Preparation of porous ceramisite for waste water treatment made from Red Mud. *Journal of Wuhan University of Technology-Materials Science Edition* **22** (1), 31–34.

Zheng, H., Liu, D. H., Zheng, Y., Liang, S. P. & Liu, Z. 2009 Sorption isotherm and kinetic modeling of aniline on Cr-bentonite. *Journal of Hazardous Materials* **167** (1–3), 141–147.

Zheng, H., Wang, Y., Zheng, Y., Zhang, H., Liang, S. P. & Long, M. 2008 Equilibrium, kinetic and thermodynamic studies on the sorption of 4-hydroxyphenol on Cr-bentonite. *Chemical Engineering Journal* **143** (1–3), 117–123.

First received 12 October 2011; accepted in revised form 26 January 2012